Article

Experimental and Discrete Element Model Investigation of Limestone Aggregate Blending Process in Vertical Static and/or Conveyor Mixer for Application in the Concrete Mixture

Lato L. Pezo [1,*] , Milada Pezo [2] , Anja Terzić [3] , Aca P. Jovanović [1] , Biljana Lončar [4] , Dragan Govedarica [4] and Predrag Kojić [4]

1   Institute of General and Physical Chemistry, University of Belgrade, Studentski Trg 12-16, 11000 Belgrade, Serbia; akiyov@gmail.com
2   Department of Thermal Engineering and Energy, "Vinča" Institute of Nuclear Sciences—National Institute of the Republic of Serbia, University of Belgrade, P.O. Box 522, 11001 Belgrade, Serbia; milada@vin.bg.ac.rs
3   Institute for Testing of Materials—IMS, Vojvode Mišića Bl. 43, 11000 Belgrade, Serbia; anja.terzic@institutims.com
4   Faculty of Technology, University of Novi Sad, Bulevar Cara Lazara 1, 21000 Novi Sad, Serbia; cbiljana@uns.ac.rs (B.L.); dragangovedarica001@gmail.com (D.G.); kojicpredrag@uns.ac.rs (P.K.)
*   Correspondence: latopezo@yahoo.co.uk; Tel.: +381-11-3283-185

Abstract: The numerical model of the granular flow within an aggregate mixture, conducted in the vertical static and/or the conveyor blender, was explored using the discrete element method (DEM) approach. The blending quality of limestone fine aggregate fractions binary mixture for application in self-compacting concrete was studied. The potential of augmenting the conveyor mixer working efficiency by joining its operation to a Komax-type vertical static mixer, to increase the blending conduct was investigated. In addition the impact of the feed height on the flow field in the cone-shaped conveyor mixer was examined using the DEM simulation. Applying the numerical approach enabled a deeper insight into the quality of blending actions, while the relative standard deviation criteria ranked the uniformity of the mixture. The primary objective of this investigation was to examine the behavior of mixture for two types of blenders and to estimate the combined blending action of these two mixers, to explore the potential to augment the homogeneity of the aggregate fractions binary mixture, i.e., mixing quality, reduce the blending time and to abbreviate the energy-consuming.

Keywords: quality optimization; self-compacting concrete; complex blending; DEM modeling

1. Introduction

Intense industrialization and urbanization that have been taking place for over a century introduced and subsequently accelerated the production of non-shaped construction materials such as concrete [1]. The numerous varieties of this non-shaped building material are being extensively utilized worldwide since concrete exhibits formidable structural properties and durability in an aggressive environment. Besides superb performances, concrete production is highly economically sustainable due to relatively cheap raw materials and its flexibility in casting [2]. However, the central part of the concrete mix design, generally comprise 60–75% of its volume [3]. Due to the high consumption and depletion of natural resources it is extremely important to consider the possibilities of optimizing of aggregate mixing [4,5] and the application of artificial aggregates as an alternative [6,7].

Self-compacting concrete (SCC) is highly workable type of concrete that can flow into various shapes and between reinforcement bars under its weight successfully filling all voids without segregation or bleeding. The aggregate plays a primary role in affecting the characteristics of fresh SCC (as it has no need for vibration to consolidate) and the final performances of the solidified composite material [8,9]. The equipment for the

granular materials mixing is broadly utilized in the process industry, including construction materials production and civil engineering [10]. The mixing process of granular materials covers their simultaneous homogenization (i.e., quality unifying) performed by scattering, convection and shear actions within the material. In addition, the mixing process is determined by particle geometries, and amounts [11]. Therefore, a better understanding of these fundamental processes within the granular material, their impact on the subsequent multi-componental blending and the mixing equipment selection is essential for mixing process management [12].

Different investigations were conducted to foresee the quality of the mixing product, such as a study by Rantanen and Khinast [13], in which the discrete element method (DEM) was applied to investigate the biopharmaceutical properties of the particle raw materials. Quite possibly, the most inventive approach to improve the blending procedure is the utilization of the DEM analysis, which could be used in the assessment of the blending conduct and its optimization [14], much faster, without a necessity to perform long, exhausting and expensive experimental procedure.

The DEM study was initially proposed by Cundall and Strack [15]. Upon this study, an extensive number of investigations affirmed this method in assessing of the particle mixing conduct in various types of blenders. Deen et al. [16] presented the hard and the soft sphere collision model frameworks to discuss the numerical implementation of these two approaches. The numerical aspects, possible prospects and results of the DEM studies performed in recent years were summarized by Zhu et al. [14]. The DEM method could be applied to evaluate significant data concerning the mixing mechanisms affected by the operating conditions for granular materials, as suggested by Huang and Kuo [17]. Gao et al. [18] investigated the effects of particle characteristics on the mixing process, and the DEM model for the contact between particles, and between blender and particles. Wang et al. [19] modeled the particle-to-particle collisions by the particle velocities and the direction of contact force, taking into account the actual densities of different parts of grains. Zhong et al. [20] used the DEM model to explore the effects of the shape of the granules in resolving the behavior of bulk solids. The impact of the particle shape and the effects of the angle of repose on the mixing dynamics were evaluated using the DEM approach by Coetzee [21]. Liu et al. [22], validated the DEM model using experiment, in which the distinction among surface and total mono-sized blending particle clusters in a rotary drum was examined.

The computational fluid dynamics (CFD) and DEM coupling approach was used to investigate the impact of particle geometry on floating behavior in a flat-bottomed spouted bed [23]. The influence of the rotation velocity on blending was explored by Liu et al. [24]. The CFD-DEM investigations were developed to study the floating behaviors of real cylindrical particles. Huaqin et al. [25], numerically simulated a gas-solid flow system with moving boundaries and modeled the wall boundaries according to the signed distance function.

The motion of three-dimensional cubic shapes granules in a thin rotating mixer is numerically simulated by Gui et al. [26]. Zhang et al. [27] applied partitioning as a technique of ranking the mixing conduct. The small-sized grain mixtures should be processed to gain a high uniformity of their content. An endeavor to better understand the system of gradual forming of dead zones during mixing, and to reach an acceptable level of mixing, varying blending variables were investigated by Asachi et al. [28]. Zheng and Yu [29], showed that increased rotation speed could significantly augment the blending result. The different influences on blending, such as rotational velocity, dosing level and the effects of the mixer's inner geometry and its contact to granules were investigated by Rong et al. [30]. The velocity field was studied for the conveyor blender and the DEM simulation was performed using GPU processors in the works by Su et al. [31]. Bimodal particle diameter distribution's influence on mixing was investigated by varying the mixing ratios of the two mixed particles [32]. The flow field of spherical granules in a mixer was calculated by

Arratia et al. [33], applying the DEM method, showing the effect of mono-disperse and bi-disperse sized material on the mixing quality.

The main idea in this investigation was to model the mixing performance of coupled vertical static and vertical-cone conveyor blenders used for homogenization of the limestone aggregate mixture. A simple vertical static mixer, with a few elements, can be used as a pre-mixer to reduce the time and to improve the final result of the blending [10]. The pre-mixer is a short, gravitationally operated, low energy mixing device, easy to handle and maintain [34]. This pre-mixer is a pipe with particular geometric elements, which influences the flow [10]. The leading idea in this study was to insert the simple, affordable pre-mixer in the mixing line in order to lower the mixing time and simultaneously increase the mixing quality. The granular material was limestone aggregate fractions, with particle diameters of $1 \div 2$, $2 \div 3$, $3 \div 4$ and $4 \div 5$ mm, and the six possible limestone aggregate mixtures were formed as a combination of different particle fractions. A set of 1, 3 or 5 Komax-type vertical static elements connected in a line was used for pre-mixing action, while the vertical-cone conveyor mixer was used as the final mixer. The quality of the mixing in the vertical static mixer was investigated in Experiment #1. The mixing capabilities within the conveyor mixer was studied in Experiment #2, while in the Experiment #3 the consequence of the coupled action of these two mixers was investigated.

2. Materials and Methods

2.1. Material Properties Determination

The limestone that was employed in this experiment was issued from the Vinići deposit, in Montenegro. According to X-ray diffraction analysis conducted on a Philips PW-1710 diffractometer with a Cu tube operated at 40 kV and 30 mA, the limestone sample was classified as calcite. The chemical composition of limestone was analyzed by atomic absorption spectroscopy (PinAAcle 900 instrument, Perkin Elmer, Boston, MA, USA). The sample was predominantly composed of CaO (56.16%). The sum of all other detected oxides was below 1%. Loss on ignition measured at 1000 °C was 42.96%. The bulk density of the experimental limestone mixture was 2705 kg/m^3.

According to the standard ore sampling campaign, a 1000 kg crude limestone sample representative for this experiment was extracted from the deposit [35]. Further processing of the crude sample included (1) initial rough crushing in a jaw crusher (KHD Humboldt Wedag; 5"–6") and (2) subsequent secondary crushing in a cone crusher (Denver Roll Crusher; 6"·10") to obtain 10 kg sub-samples. The smallest grain fractions were obtained in an agate stone mill (KHD Humboldt Wedag). Six pairs of binary mixtures with different particle diameters were investigated within this study: $(1 \div 2$ mm$/2 \div 3$ mm$)$; $(1 \div 2$ mm$/3 \div 4$ mm$)$; $(1 \div 2$ mm$/4 \div 5$ mm$)$; $(2 \div 3$ mm$/3 \div 4$ mm$)$; $(2 \div 3$ mm$/4 \div$ mm$)$ and $(3 \div 4$ mm$/4 \div 5$ mm$)$. The targeted grain-distribution was obtained via sieve analysis.

2.2. Calculation of the RSD Criterion

The homogeneity of the limestone binary mixture was assessed by the *RSD* criteria, both for experimental and numerical simulation, as proposed by Poux et al. [36]:

$$RSD = \frac{\sigma}{\bar{x}} \cdot 100\%, \ \sigma = \sqrt{\frac{\sum\limits_{i=1}^{M} (\bar{x} - x_i)^2}{M - 1}}, \tag{1}$$

where: M is the number of samples, x_i—the frequency of the specific colour occurrence in a sample i and $\bar{x}$—the average frequency of the specific colour occurrence in all samples.

The colour photos were captured using a Nikon Digital SLR Camera D7100. The acquired photos were recorded in high resolution, effective 24.1 million pixels, 23.5×15.6 mm, with complementary metal–oxide–semiconductor (CMOS) sensor. These digital pictures were split into 4 parts (as mentioned in the paper by Pezo et al. [11]), while the rate of colored particle occurrence was calculated for each quadrant.

2.3. Experiment #1

The experimental Komax-type vertical static mixer (1, 3 or 5 elements connected in a sequential row), which was used in this study, was made of transparent Plexiglas pipe (diameter 60 mm) [10], while the internal geometry of the mixer was 3D printed. The three elements at the vertical static mixer are illustrated in Figure 1. The numerically obtained particle paths are also presented in Figure 1. Each blending element (in the height of 60 mm) was rotated by the axis by 90° concerning the preceding segment, with the idea to diversify the flow of particles falling gravitationally from the preceding segment into two particle flows and allow the mixing in the next blending element.
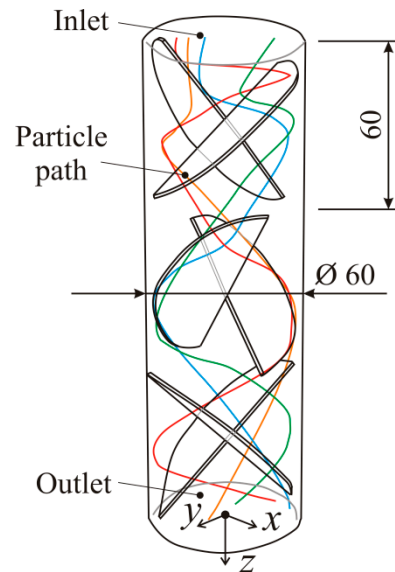

Figure 1. Komax-type vertical static mixer, with three blending elements.

In order to simplify the visual access to the mixing process, the limestone particles were painted in yellow, red, blue and green (particles were in size of: $1 \div 2$, $2 \div 3$, $3 \div 4$ and $4 \div 5$ mm, respectively), Figure 2a. The inlet of the Komax-type vertical static mixer is located in the upper segment, which is divided into two compartments (50% of space for blue; 50% for yellow particles. The mixing results of the vertical static mixer for mixing $1 \div 2$ and $2 \div 3$ mm particles were presented in Figure 2b (static mixer with three mixing elements) and Figure 2c (five mixing elements).
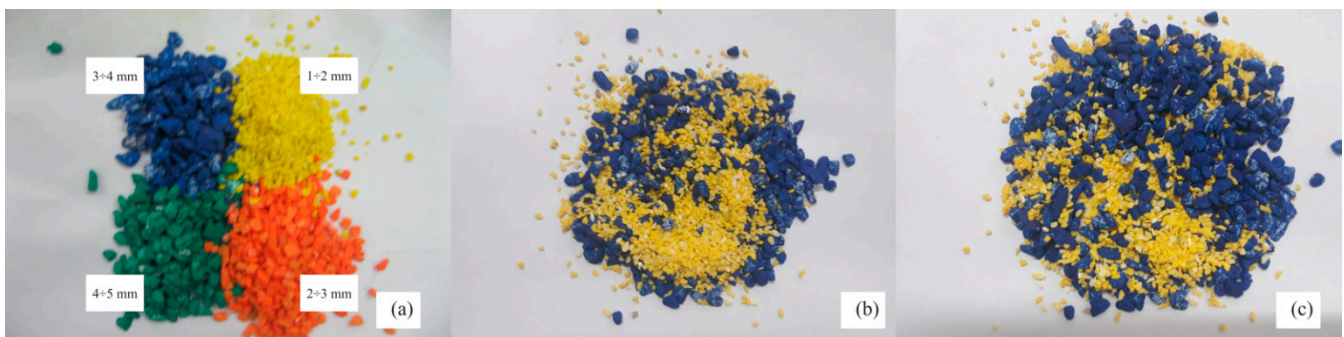
Figure 2. The blending material used for blending experiments (**a**), the blending conduct, (binary mixture of limestone particles, diameters $1 \div 2$ and $3 \div 4$ mm), after pre-mixing with three elements, (**b**), following the vertical static mixer equipped with five elements (**c**).

In Experiment #1, the binary mixture (painted limestone particles) passed gravitationally via vertical static mixer with 1, 3 or 5 elements (Figure 1). The RSD values,

obtained from the Equation (1) were calculated. The mass of the batch was 4–5 kg, for each experiment. The determined RSD value was calculated as a mean for 10 samples.

2.4. Experiment #2

In Experiment #2, the conveyor blender with an embedded vertical screw conveyor, constructed in the transparent Plexiglas, was applied to execute the mixing action, Figure 3a. The basic technological data of the applied blender was presented in Figure 3b. The granules remaining time in the blender vessel is 4, 12 or 20 min, the relative standard deviation for blending operation reached 45–55% (after 20 min). The length of the vertical screw was 500 mm, while the screw conveyor casing diameter was equal to 50 mm. The rotation of the screw conveyor was realized manually (10 rpm). The batch size in the experiments reached between 4 and 5 kg. At the same time, the mixing efficiency (expressed by the RSD value) was calculated after 4, 12 or 20 min of mixing duration (precisely 10 samples of 50 g estimated weights were picked up from each batch). Samples were taken at the outlet of the cone of the conveyor mixer (Figure 3b,c).
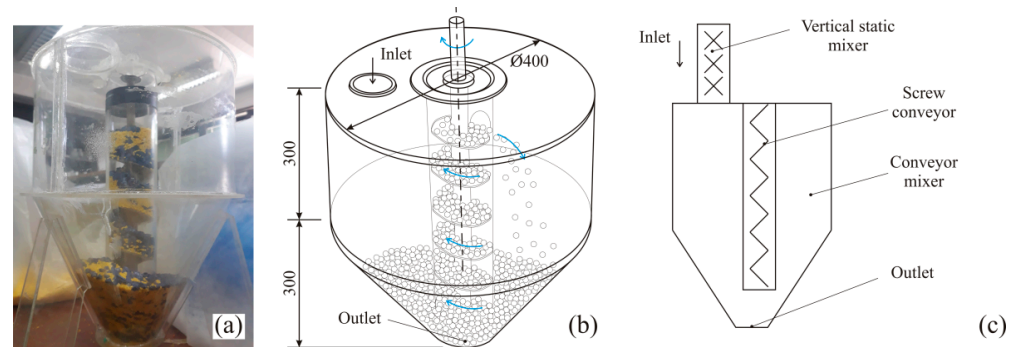

Figure 3. Conveyor mixer used in the experiment of the binary mixture (painted limestone particles) particle, used for mixing experiments (**a**), the scheme of mixing principle (**b**), coupling of vertical static mixer and conveyor mixer (**c**).

The effect of the feed layer height on the particle flow inside the conveyor mixer was performed in Experiment #2. The falling trend of particles velocities inside the conveyor mixer was anticipated according to DEM analysis. Particles motion almost followed the first-in- first-out principle within the mixer, however, this order of packing was not ensured due to the ununiform dispersion of the flow field. Therefore, the drawdown index (DI) was introduced to equate and assess the particle model coherence inside the conveyor mixer. The DI parameter was utilized to disclose and assess the flow field of the particles, calculating the average divergence of the normally distributed extent in the z-axis direction. The calculation of the *DI* parameter was described in details by Han, et al. [37]:

$$DI = \frac{1}{m} \cdot \sum_{i=1}^{m} \sqrt{\frac{\sum_{j=1}^{n} \left(V'_{ij} - \overline{V'_i} \right)^2}{n-1}}, \quad V'_{ij} = \frac{V_{ij} - V_{\min}}{V_{\max} - V_{\min}}, \quad \overline{V'_i} = \frac{1}{n} \sum_{j=1}^{n} V'_{ij} \quad (2)$$

where: V'_{ij} is the normal velocity of a cell in the particle layer, at row *i*, column *j*; V_{ij} is the mean velocity magnitude of a cell at row *i*, column *j*; $V_{\min}$ and $V_{\max}$ are the minimum and maximum of the mean velocity magnitude, accordingly; *m* and *n* are the number of layers and the number of columns, respectively.

2.5. Experiment #3

This experiment was performed in the conveyor mixer, as described in the previous experiment, applying the same granular material (the binary mixture of painted limestone particles), but processed before in the vertical static mixer, with 5 mixing elements (as

mentioned in Experiment #1). The scheme of the coupling of vertical static mixer and conveyor mixer was presented in Figure 3c. The mixing duration inside the upward blender was abbreviated to a 3/4 time period of Experiment #2, after the material passed through the vertical static mixer.

2.6. The Mathematical Model

The DEM model was simulated to foresee the blending results of the vertical static element elements (such as Komax vertical static mixer), the conveyor blender, and in the case of coupled action of these mixers. The conduct of the DEM calculation for the three sets of experiments was matched with the experimental study results, having in mind the whole blending process. The impact of the fluid stream on the aggregate behavior was considered negligible, and was dismissed from the calculation, because the pressure losses and the air velocities were low. The DEM study was performed according to the same parameters as those recorded in the experiments.

2.7. The Vertical Static Mixer Model

According to the literature [12,14], the contact between two mixing particles was regarded as the contact among two inflexible entities, these items were allowed to be somewhat superimposed in the computation. The linear spring–dashpot model was utilized in the simulation, as suggested by Cundall and Strack [15]. The contact force amidst two particles was split into tangential and normal projections. As mentioned in the DEM model, the movement of a particle i at the time t, can be calculated using the Newton's law of motion:

$$m_i \frac{dv_i}{dt} = f_{p-f,i} + \sum_{j=1}^{k_i} \left(f_{c,ij} + f_{d,ij} \right) + m_i g \tag{3}$$

$$I_i \frac{d\omega_i}{dt} = \sum_{j=1}^{k_i} \left(T_{ij} + M_{ij} \right) \tag{4}$$

where: m_i, I_i, v_i and ω_i denote the mass, moment of inertia, translational and rotational velocities of particle i, accordingly.

The forces among particles i and j, encompass the contact forces, $f_{c,ij}$, viscous damping forces, $f_{d,ij}$, and the gravitational force, $m_i \cdot g$. They were outlined thoroughly by Cundall and Strack [15]. The normal force (F_n) was estimated, based on the degree of particle overlap (α):

$$F_n = k_1 \alpha \ (\alpha \text{ increasing}) \tag{5}$$

$$F_n = k_2 (\alpha - \alpha_0) \ (\alpha \text{ decreasing}) \tag{6}$$

k_1 and k_2 denote stiffness constants, and α_0, was the value of the overlap at zero normal force.

The tangential force (Ft) was evaluated applying the Hertz model, outlined in Walton and Braun model [38]. The extent of Ft was calculated based on the tangential slip amount in the last time step and the record of the contact, which is constrained by the coefficient of friction, μ as:

$$F_t = \mu F_n \tag{7}$$

where μ is the friction coefficient.

The sensing of contact between particles and helix enforces the highest computational load of the DEM calculus, according to the complex helix geometry. The initial moment of the DEM calculation was in at the moment when a particle accessed the vertical static mixer and the end of the trajectory was observed at the end of the mixer.

The contact between particles throughout the conveyance of granules was realized in a geometrically defined contact zone shaped by the deformation of the particles [20]. The contact force could be presented with two components: normal and tangential projection.

The DEM analysis embraces a rapid, numerically fast, relatively straightforward, mainly linear models and equations for evaluate the enforced forces and torques emerging by the contact between particles. The most frequent linear model, applied extensively in DEM simulations, is the linear spring–dashpot model [21], in which the spring explains the elastic deformation, while the dashpot clarifies the viscous dissipation.

The material and numerical parameters used in the DEM analysis are presented in Table 1.

Table 1. Parameters of the material and numerical parameters, used in the modelling process.

Parameter	Value
Number of particles	100,000
Particle diameters	$1 \div 2$; $2 \div 3$; $3 \div 4$ or $4 \div 5$ mm
Time step	5×10^{-6} s
Angle of repose	$41°$
Particle friction	0.35
Rolling friction	0.33
Particle-to-wall friction coefficient	0.29
Particle elastic coefficient	0.33
Particle-to-wall elastic coefficient	0.32
Particle damping coefficient	0.26
Particle-to-wall damping coefficients	0.27
Restitution coefficient	0.54
Poisson's ratio of particles	0.26
Young's modulus	107

2.8. Description of Screw Conveyor

A simulation of a bulk material transport through a horizontal screw conveyor is presented in a study by Kretz et al. [39], in which the common problems in practical applications of screw conveyors, and the uneven material (limestone aggregate mixture) flow in time was investigated, through the variations in product quality and certain gaps in the knowledge in theoretical solutions. The cylindrical coordinates were applied for the parametric designation of a helix surface to evaluate the 3D-geometric constraints numerically [40]. The necessary simplification of the helix geometry was implemented in the calculation, using the adequate screw surface model:

$$\vec{r}(\theta) = R \cdot \cos\theta \cdot \vec{i} + R\sin\theta \cdot \vec{j} + \frac{p}{2\pi} \cdot \theta \cdot \vec{k} \qquad (8)$$

where p is the pitch of a helix, R radius and θ angle from x-axis to x-y plane.

3. Results and Discussion

3.1. Experiment #1

Particle paths of four particles obtained by the DEM study were presented in Figure 1. These particles were picked randomly, each taken from one of the four quadrants of the circular section. In addition, a Poincare plot is utilized to present the path of the particles within the sections in the vertical static mixer. The Poincare plot locates a colored dot for each particle at the position at which the particle passes through a cut plane (termed as a Poincare section). In Figure 4, the positions of particles at six different Poincare segments in the vertical static mixer were presented at heights: $0 \cdot H$, $0.5 \cdot H$, $1 \cdot H$, $1.5 \cdot H$, $2 \cdot H$ and $3 \cdot H$. The color parameter is a logical expression employed to mark the initial color of particles at positions $x < 0$ (yellow) and $x > 0$ (blue). As the particles start to follow the flow of particles,

they start to blend. By the end of the mixer, the particles have not blend totally—there are critical pockets of just yellow and blue particles to be mixed more appropriately.
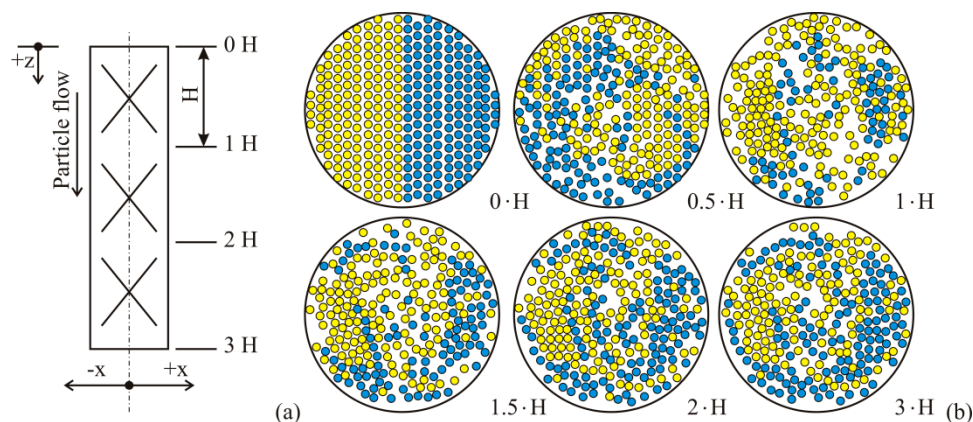

Figure 4. Three-element vertical static mixer scheme. (**a**) Poincare maps of the particle trajectories from different Poincare sections in the three-element vertical static mixer (H—mixing element height) (**b**).

The relative standard deviation values decayed in all three sets of trials and accompanied numerical studies, for all three experimental groups. The quality of mixing was augmented with the increase in the count of blending elements within a vertical static mixer. The contrast between the experimental and the DEM model results (presented as RSD values) is illustrated in Figure 5 (for Experiment #1), which outlined the obtained conduct of the performed experiment.

The DEM approach was applied to investigate particle motions throughout the mixing procedure, involving particle mechanics (tracking, location and movement) in the three Cartesian dimensions. The position of the specific particle is fundamentally varied through blending, with the expressive changes in mechanics parameters (position, velocity, and acceleration), which provide the potential to enhance the mixing quality [10,41].

The uniformity result acquired following after the passage of the limestone aggregate mixture particles through only one element of the vertical static mixer exhibited the RSD values of 90.68; 94.50; 95.78; 91.23; 91.65 and 90.28%, for binary mixture: (1 ÷ 2 mm)—(2 ÷ 3 mm), (1 ÷ 2 mm)—(3 ÷ 4 mm), (1 ÷ 2 mm)—(4 ÷ 5 mm), (2 ÷ 3 mm)—(3 ÷ 4 mm), (2 ÷ 3 mm)—(4 ÷ mm) and (3 ÷ 4 mm)—(4 ÷ 5 mm), respectively, which went far beyond the recommended value of 10% [41]. The acquired result of the DEM investigation showed almost the same results, indicating the RSD value of 90.26; 98.79; 99.57; 87.24, 89.07, and 93.87%, respectively for the above-mentioned limestone aggregate mixture.

The uniformity of a limestone aggregate mixture falling through a vertical static mixer equipped with 1, 3 or 5 elements illustrated a declining trend of RSD value specifying the better mixing action, but the goal of RSD < 10% was not nearly fulfilled. Besides, Figure 5 expressed the dependence of RSD value and the count of passages through the vertical static mixer, for the experimental and the numerical study. The RSD could be lowered, by boosting the mixing elements count, but not enough to reach the level below 10%. In addition, by increasing the blending parts count, the structure of the vertical static mixer could induce the augment in the installing investments [11]. Figure 5 also demonstrated that numerical results agreed with trial conduct, cross-referenced the acquired RSD values (r^2 was 0.968).
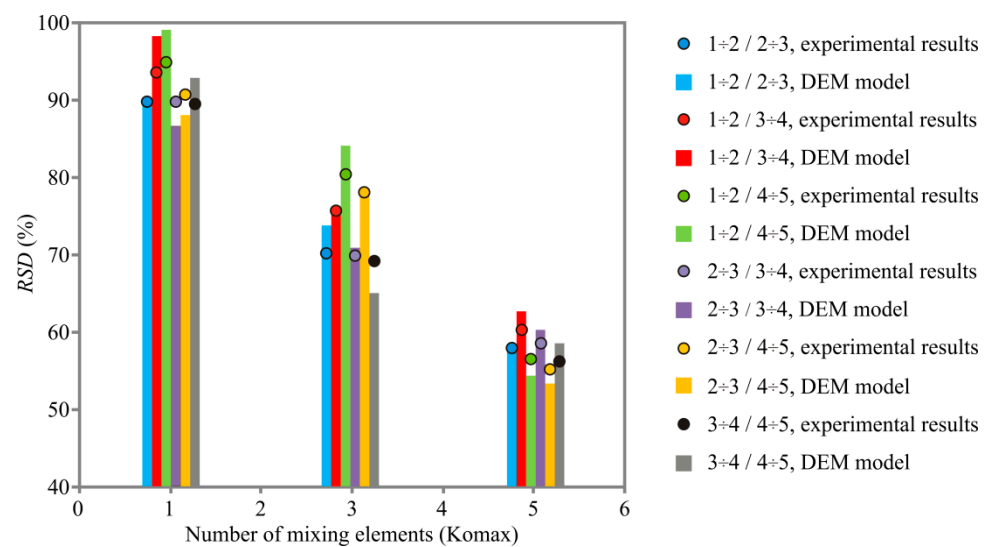
Figure 5. The RSD estimation for Experiment #1.

3.2. Experiment #2

The investigation of the possible opportunities to diminish the relative statistic deviation in the conveyor mixer was accomplished in Experiment #2. The mixing duration throughout the conveyor mixer was set to: 4, 12 or 20 min, and the outcomes of the uniformity tests were discovered by the RSD criteria evaluation, Figure 6.
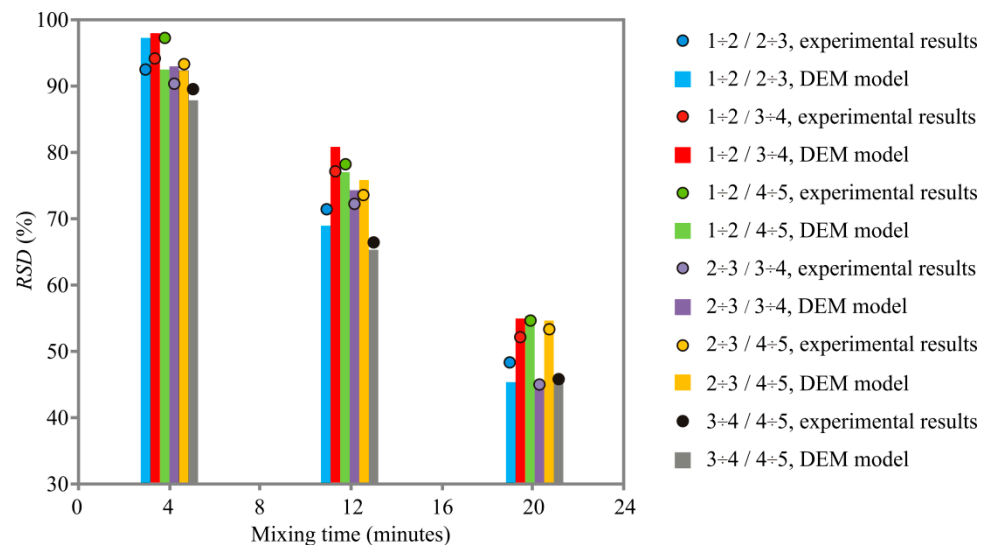

Figure 6. The RSD results in Experiment #2.

After mixing in the conveyor mixer, the uniformity results estimation of the limestone aggregate mixture (which did not fall beforehand through the vertical static mixer) explained that RSD were between 45.10 and 54.76%, after 20 min, for experimental and between 45.25 and 55.60% for the DEM simulation, respectively, vertical static mixer. The uniformity plateau was not accomplished [41]. In Figure 6, the similarity of the conduct acquired in the trial study and the conduct using the DEM calculation was presented, while the acquired r^2 value between experimental and DEM results was equal to 0.983.

3.3. Particle Flow Field throughout the Conveyor Mixer

The effect of the feed height on the flow field for the conveyor mixer was investigated in Experiment #2, using the DEM calculation. The height of the particle feed was set to 400, 450 and 500 mm. During the mixing, the material was taken from the bottom of the cone

part using the central screw conveyor and continuously transferred to the top of the mixer, where it fell gravitationally (Figure 3b). Figure 7 explained the velocity field allocation for distinct heights of feed. The downward stream and a clockwise deviation in velocity magnitude were monitored in three cases of feed height (400, 450 and 500 mm), Figure 7. Velocity magnitudes and velocity vectors of particles positioned at higher levels showed reduced values. With the augment of feed height, a substantial growth in the downward velocities of particles in the whole hopper could be observed, which collides with the results of Han, et al. [37].
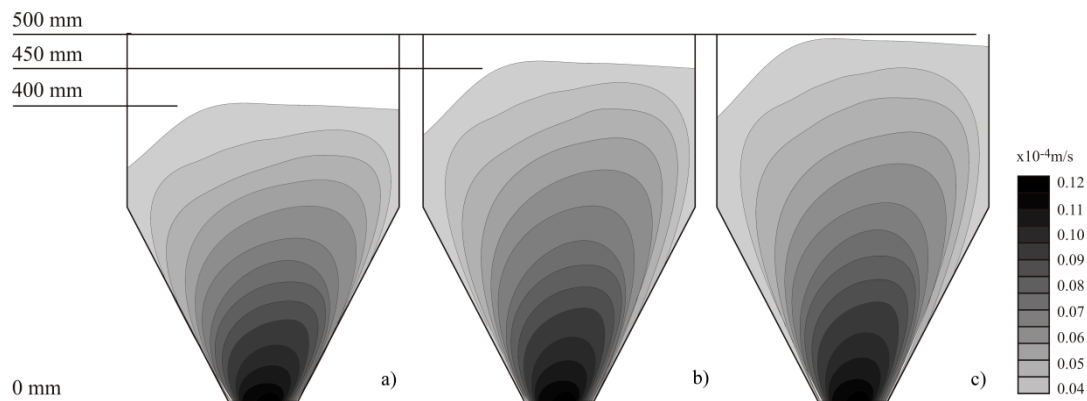

Figure 7. Distributions of the particle stream with distinct heights in the hopper of the conveyor mixer, in case of feed height: (**a**) 400 mm; (**b**) 450 mm and (**c**) 500 mm.

3.4. Experiment #3

In Experiment #3, the limestone aggregate mixture, was previously mixed using the Komax-type vertical static mixer equipped with five elements (in Experiment #1), was blended in the conveyor mixer. An attempt was made to improve the result and shorten the blending duration to 3/4 of that time applied for Experiment #2. The blending duration was set to 3, 9 or 15 min, in Experiment #3.

The conduct acquired in this experiment was given in Figure 8, and the results show an increase in the blending outcome, with the simultaneous reduction in the mixing duration (RSD value reached the level between 3.34 to 13.79 after 15 min for the experimental investigations and 3.50—13.95%, after 15 min, for DEM study. Thus, all three blending periods in Experiment #3 were shortened to 3/4 of the periods obtained in Experiment #2, with the RSD values reduced. However, the required uniformity plateau was not accomplished for all mixtures, after 15 min, and the mixing period should be increased to 20 for 1 ÷ 3 mm limestone aggregate mixture, or even 25—30 min for 1 ÷ 4 mm or 2 ÷ 4 mm limestone aggregate mixture. These outcomes provoked the decision that less engagement and the minor effort of the final blender in the line could be required, if a vertical static mixer was applied prior to the principal mixer.

Figure 8 shows the RSD value for the mixing duration of the experiment and DEM simulation results. It was obvious that as the blending duration increased, the RSD value diminished. The similarity of the results of the experimental investigation and the DEM study, regarding the blending quality calculation is evident, as was the case in the previous sets of experiments (obtained r^2 was 0.995).
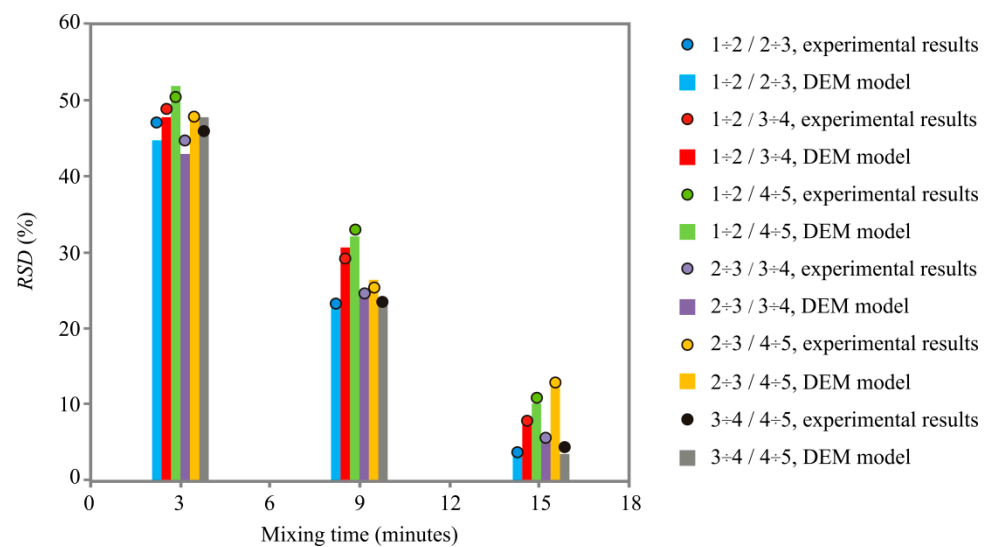
Figure 8. The RSD results obtained in Experiment #3.

4. Conclusions

Within this manuscript, an experimental study and the discrete element method (DEM) were performed to investigate the homogenization process of the fine limestone aggregate used for self-compacting concrete mixtures in the vertical static mixer (type Komax), the conveyor mixer and the coupled action of these mixers. The crucial point of this examination was to study the potential outcomes to construct an affordable, easy to manufacture, uncomplicated device, which could be inserted in the blending line, with a goal to expand the final quality of the mixing process and lower the mixing time. This task was investigated through experimental and numerical study, using the DEM approach.

Three experiments were considered. The blending was performed using the vertical static mixer, with one, three or five elements, in the initial experiment. The optimal outcome was accomplished with five mixing parts, according to the RSD criteria. Notwithstanding, the mixing conduct was unsuitable, which was concluded by the RSD value greater than 10%. In Experiment #2 the mixing process in the conveyor blender was examined, and the outcome of the process was estimated according to the blending duration. The inadequate RSD value between 45.10 and 54.76%, for experimental and between 45.25 and 55.60% for the DEM model, respectively for trials study and the DEM simulation, accordingly was managed after 20 min.

The limestone aggregate mixture was previously homogenized in the vertical static mixer, encompassing five elements, in the final experiment. The mixing process was executed in the conveyor mixer, and the mixing duration in Experiment #3 was shortened to only 3/4 of the duration in the preceding trials. The results of Experiment #3 exhibited that the RSD plateau was reached after only 15 min of mixing, for the mixtures with similar particle diameters. However, the mixtures composed of higher differences in particle diameter (such as $1 \div 4$, $2 \div 4$ or $1 \div 3$ mm mixtures) were not thoroughly mixed (RSD was not underneath 10%), after 15 min, even if the vertical static mixer was used for pre-mixing. However, the additional decrease of the RSD value could be accomplished with a longer duration of the blending process.

According to the results of the study, the DEM simulation can be included in the improvement of the mixing equipment configuration. It is a reliable, trustworthy numerical tool, accurate and satisfactory method in estimating the parameters of the blending process, but the experimental trials were required for approval and confirmation of these strategies. In addition, the anticipation of the limestone aggregate behavior in vertical static and conveyor mixers and subsequent optimization of the combined mixing action of two mixers using analytical modeling impacts the increasing homogeneity of the limestone aggregate mix for self-compacting concrete and improves the sustainability of SCC produc-

tion by shortening the mixing time and reducing the energy consumption necessary for the mixing procedure.

Author Contributions: Conceptualization, L.L.P., M.P. and A.P.J.; methodology, L.L.P., M.P. and A.P.J.; software, A.P.J.; validation, B.L., D.G. and P.K.; formal analysis, L.L.P. and A.P.J.; investigation, A.P.J.; resources, A.T.; data curation, L.L.P.; writing—original draft preparation, L.L.P., M.P. and A.T.; writing—review and editing, L.L.P., M.P., A.T. and B.L.; visualization, L.L.P.; supervision, D.G.; project administration, L.L.P.; funding acquisition, L.L.P., M.P. and B.L. All authors have read and agreed to the published version of the manuscript.

Institutional Review Board Statement: Not applicable.

Informed Consent Statement: Not applicable.

Data Availability Statement: Not applicable.

Conflicts of Interest: The authors declare no conflict of interest.

References

1. Wang, R.; Yu, N.; Li, Y. Methods for improving the microstructure of recycled concrete aggregate: A review. *Construct. Build. Mater.* **2020**, *242*, 118164. [CrossRef]
2. Rashid, K.; Rehman, M.; de Brito, J.; Ghafoor, H. Multi-criteria optimization of recycled aggregate concrete mixes. *J. Clean. Prod.* **2020**, *276*, 124316. [CrossRef]
3. Rehman, U.M.; Rashid, K.; Ul Haq, E.; Hussain, M.; Shehzad, N. Physico-mechanical performance and durability of artificial lightweight aggregates synthesized by cementing and geopolymerization. *Construct. Build. Mater.* **2020**, *232*, 117290. [CrossRef]
4. Chu, S.H.; Poon, C.S.; Lam, C.S.; Li, L. Effect of natural and recycled aggregate packing on properties of concrete blocks. *Construct. Build. Mater.* **2021**, *278*, 122247. [CrossRef]
5. Al-Tersawy, S.H.; El-Sadany, R.A.; Sallam, H.E.M. Experimental gamma-ray attenuation and theoretical optimization of barite concrete mixtures with nanomaterials against neutrons and gamma rays. *Construct. Build. Mater.* **2021**, *289*, 123190. [CrossRef]
6. Habibi, A.; Ramezanianpour, A.M.; Mahdikhan, M. RSM-based optimized mix design of recycled aggregate concrete containing supplementary cementitious materials based on waste generation and global warming potential. *Resour. Conserv. Recycl.* **2021**, *167*, 105420. [CrossRef]
7. Tam, V.W.Y.; Tam, C.M.; Wang, Y. Optimization on proportion for recycled aggregate in concrete using two-stage mixing approach. *Construct. Build. Mater.* **2007**, *21*, 1928–1939. [CrossRef]
8. Sayed Ali, Z.; Hosseinpoor, M.; Yahia, A. New aggregate grading models for low-binder self-consolidating and semi-self-consolidating concrete (Eco-SCC and Eco-semi-SCC). *Construct. Build. Mater.* **2020**, *265*, 120314. [CrossRef]
9. Li, N.; Long, G.; Ma, C.; Fu, Q.; Zeng, X.; Ma, K.; Xie, Y.; Luo, B. Properties of self-compacting concrete (SCC) with recycled tire rubber aggregate: A comprehensive study. *J. Clean. Prod.* **2019**, *236*, 117707. [CrossRef]
10. Jovanović, A.; Pezo, M.; Pezo, L.; Lević, L. DEM/CFD analysis of granular flow in static mixers. *Powder Technol.* **2014**, *266*, 240–248. [CrossRef]
11. Pezo, M.; Pezo, L.; Jovanović, A.; Lončar, B.; Čolović, R. DEM/CFD approach for modeling granular flow in the revolving static mixer. *Chem. Eng. Res. Des.* **2016**, *109*, 317–326. [CrossRef]
12. Lemieux, A.; Leonard, G.; Doucet, J.; Leclaire, L.A.; Viens, F.; Chaouki, J. Large-scale numerical investigation of solids mixing in a V-blender using the discrete element method. *Powder Technol.* **2008**, *181*, 205–216. [CrossRef]
13. Rantanen, J.; Khinast, J. The future of pharmaceutical manufacturing sciences. *J. Pharm. Sci.* **2015**, *104*, 3612–3638. [CrossRef]
14. Zhu, H.P.; Zhou, Z.Y.; Yang, R.Y.; Yu, A.B. Discrete particle simulation of particulate systems: A review of major applications and findings. *Chem. Eng. Sci.* **2008**, *63*, 5728–5770. [CrossRef]
15. Cundall, P.A.; Strack, O.D.L. A discrete numerical model for granular assemblies. *Géotechnique* **1979**, *29*, 47–65. [CrossRef]
16. Deen, N.G.; Van Sint Annaland, M.; Van der Hoef, M.A.; Kuipers, J.A.M. Review of discrete particle modeling of fluidized beds. *Chem. Eng. Sci.* **2007**, *62*, 28–44. [CrossRef]
17. Huang, A.-N.; Kuo, H.-P. Developments in the tools for the investigation of mixing in particulate systems—A review. *Adv. Powder Technol.* **2014**, *25*, 163–173. [CrossRef]
18. Gao, W.; Wang, J.; Yin, S.; Feng, Y.T. A coupled 3D isogeometric and discrete element approach for modeling interactions between structures and granular matters. *Comput. Methods Appl. Mech. Eng.* **2019**, *354*, 441–463. [CrossRef]
19. Wang, L.; Wu, B.; Wu, Z.; Li, R.; Feng, X. Experimental determination of the coefficient of restitution of particle-particle collision for frozen maize grains. *Powder Technol.* **2018**, *338*, 263–273. [CrossRef]
20. Zhong, W.; Yu, A.; Liu, X.; Tong, Z.; Zhang, H. DEM/CFD-DEM modelling of non-spherical particulate systems: Theoretical developments and applications. *Powder Technol.* **2016**, *302*, 108–152. [CrossRef]

21. Coetzee, C.J. Review: Calibration of the discrete element method. *Powder Technol.* **2017**, *310*, 104–142. [CrossRef]
22. Liu, X.; Hu, Z.; Wu, W.; Zhan, J.; Herz, F.; Specht, E. DEM study on the surface mixing and whole mixing of granular materials in rotary drums. *Powder Technol.* **2017**, *315*, 438–444. [CrossRef]
23. Li, L.; Kemp, I.; Palmer, M. A DEM-based mechanistic model for scale-up of industrial tablet coating processes. *Powder Technol.* **2020**, *364*, 698–707. [CrossRef]
24. Liu, X.; Gan, J.; Zhong, W.; Yu, A. Particle shape effects on dynamic behaviors in a spouted bed: CFD-DEM study. *Powder Technol.* **2020**, *361*, 349–362. [CrossRef]
25. Huaqin, Y.; Yuki, M.; Kazuya, T.; Xiaosong, S.; Mikio, S. Numerical investigation on the influence of air flow in a die filling process. *J. Taiwan Inst. Chem. Eng.* **2018**, *90*, 9–17.
26. Gui, N.; Yang, X.; Tu, J.; Jiang, S. Numerical study of the motion behaviour of three-dimensional cubic particle in a thin drum. *Adv. Powder Technol.* **2018**, *29*, 426–437. [CrossRef]
27. Zhang, Z.; Gui, N.; Ge, L.; Li, Z. Numerical study of mixing of binary-sized particles in rotating tumblers on the effects of end-walls and size ratios. *Powder Technol.* **2017**, *314*, 164–174. [CrossRef]
28. Asachi, M.; Nourafkan, E.; Hassanpour, A. A review of current techniques for the evaluation of powder mixing. *Adv. Powder Technol.* **2018**, *29*, 1525–1549. [CrossRef]
29. Zheng, Q.J.; Yu, A.B. Modelling the granular flow in a rotating drum by the Eulerian finite element method. *Powder Technol.* **2015**, *286*, 361–370. [CrossRef]
30. Rong, W.; Feng, Y.; Schwarz, P.; Witt, P.; Li, B.; Song, T.; Zhou, J. Numerical study of the solid flow behavior in a rotating drum based on a multiphase CFD model accounting for solid frictional viscosity and wall friction. *Powder Technol.* **2020**, *361*, 87–98. [CrossRef]
31. Su, J.; Chai, G.; Wang, L.; Cao, W.; Gu, Z.; Chen, C.; Xu, X.Y. Pore-scale direct numerical simulation of particle transport in porous media. *Chem. Eng. Sci.* **2019**, *199*, 613–627. [CrossRef]
32. Tsunoyama, T.; Yoshida, M.; Shimosaka, A.; Shirakawa, Y. Effects of mixing ratio and order of admixed particles with two diameters on improvement of compacted packing fraction. *Adv. Powder Technol.* **2020**, *31*, 2430–2437. [CrossRef]
33. Arratia, P.E.; Duong, N.-H.; Muzzio, F.J.; Godbole, P.; Reynolds, S. A study of the mixing and segregation mechanisms in the Bohle Tote blender via DEM simulations. *Powder Technol.* **2006**, *164*, 50–57. [CrossRef]
34. Montante, G.; Coroneo, M.; Paglianti, A. Blending of miscible liquids with different densities and viscosities in static mixers. *Chem. Eng. Sci.* **2016**, *141*, 250–260. [CrossRef]
35. Annels, A.E. Mine sampling. In *Mineral Deposit Evaluation*; Springer: Dordrecht, The Netherlands, 1991.
36. Poux, M.; Fayolle, P.; Bertrand, J. Powder mixing: Some practical rules applied to agitated systems. *Powder Technol.* **1991**, *68*, 213–234. [CrossRef]
37. Han, Y.; Jia, F.; Zeng, Y.; Jiang, L.; Zhang, Y.; Cao, B. DEM study of particle conveying in a feed screw section of vertical rice mill. *Powder Technol.* **2017**, *311*, 213–225. [CrossRef]
38. Walton, O.R.; Braun, R.L. Viscosity, granular-temperature, and stress calculations for shearing assemblies of inelastic frictional disks. *J. Rheol.* **1986**, *30*, 949–980. [CrossRef]
39. Kretz, D.; Callau-Monje, S.; Hitschler, M.; Hien, A.; Raedle, M.; Hesser, J. Discrete element method (DEM) simulation and validation of a screw feeder system. *Powder Technol.* **2016**, *287*, 131–138. [CrossRef]
40. Yan, Z.; Wilkinson, S.K.; Stitt, E.H.; Marigo, M. Discrete element modelling (DEM) input parameters: Understanding their impact on model predictions using statistical analysis. *Comput. Part. Mech.* **2015**, *2*, 283–299. [CrossRef]
41. Pezo, L.; Pezo, M.; Banjac, V.; Jovanović, A.P.; Krulj, J.; Kojić, J.; Kojić, P. Blending performance of the coupled Ross static mixer and vertical feed mixer—Discrete element model approach. *Powder Technol.* **2020**, *375*, 20–27. [CrossRef]